Experiment 6 & 7:
Harmonic Oscillator - Physical Pendulum and Waves on a Vibrating Spring

Mihir Mathur
204 612 694

Section: Lab 15, Thursday 2pm
Date: 5/19/2016 and 5/26/2016
TA: Krishna Choudhary
Lab Partners: Michael Arreola-Zamora, Jonathan Zatur

Investigating Harmonic Oscillation of a Physical Pendulum and Waves on a vibrating spring

Mihir Mathur[1]

In mechanics, a physical pendulum is any rigid body that is free to rotate about a pivot. A physical pendulum undergoes a harmonic oscillation if it is given a slight amplitude about its equilibrium position. Harmonic motion is also exhibited by non-rigid systems like vibrating strings where each particle on the wave oscillates periodically. The first objective of this experiment was to investigate the oscillation of a physical pendulum in the frequency domain by studying the underdamped, overdamped and critically damped motion and to thus get a better understanding of control systems for physics applications. For analyzing these motions, an aluminum pendulum along with a wave driver and damping magnets were used and graphs were plotted for the motions. The resonant frequency for driven oscillation was found to be $.743 \pm .0005 Hz$. The second objective was to measure the velocity of waves on a vibrating string, observe modes of standing wave oscillation and study the effects of adding a boundary condition to a vibrating string in the middle of the string. The wave speed was calculated for different values of hanging masses and the frequency of the fundamental mode was calculated to be $8.335 \pm .0005$ Hz.

[1]Henry Samueli School of Engineering and Applied Science, University of California Los Angeles

Introduction

Harmonic oscillations are found in nature and this topic was studied by scientists like Robert Hooke and Jean Fourier. A physical pendulum undergoes a harmonic oscillation about its equilibrium position due to an initial displacement and its inertia. An anchor-shaped aluminum pendulum can be used as a physical pendulum to study the damping regimes—damped, undamped and critically damped oscillation. For controlling and tuning the damping force, movable magnets, positioned on opposite sides of the pendulum, are used to provide damping by Eddy current heating. The three domains of harmonic motion are:

1) Underdamped Motion: Case when there is oscillation for 0 initial velocity. Occurs when oscillation frequency is higher than damping rate.
2) Overdamped Motion: Occurs when oscillation frequency is lower than damping rate.
3) Critically Damped Motion: Case when system returns to equilibrium state fastest. Occurs when oscillation frequency is equal to damping rate.

For studying the harmonic motion with driving, a sinusoidal driving torque is produced on the pendulum by the wave driver. Furthermore, Lissajous Figures or parametric plots between pendulum angle and drive voltage are used to predict the resonance frequency. The graph of oscillation amplitude for different values of driving frequency is called the resonance curve.

A vibrating spring is a non-rigid system that demonstrates harmonic motion. Each particle on the vibrating spring oscillates periodically in relation with the adjacent particles. For this experiment, an actuator was used to provide vertical oscillations to a thick string. For analyzing the motion of the wave, a laser light is scattered into a photodetector by positioning the equipment such that the laser light lit the top of the string in rest condition. The wave velocity can be measured by calculating the linear mass density for various tensions and observing the graph for a pulse moving on the string. Furthermore, the resonant frequency for a wave on a vibrating string is the frequency which produces maximum amplitude and this can be found using Lissajous figures. The effects of boundary conditions on a vibrating string are also investigated for studying harmonic motion.

Methods

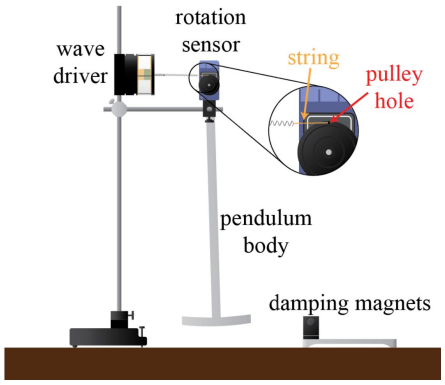

Figure 6.1 Experimental setup for studying the three different damping regimes for a physical pendulum[1].

For the first part of the experiment, the pendulum, wave driver, rotation sensor and damping magnets were setup as shown in Figure 6.1. The heights of the posts and clamps were adjusted such that the pendulum could rotate freely. Since the oscillating frequency is independent of amplitude for small amplitudes, the pendulum should be able to move a couple of inches above the table. The wave driver and rotation sensor were connected to the DAQ. A photogate was also attached to determine the starting time of the run. The sampling rate was set to 50Hz on the program to get enough data points. The mode was set to continuous and rotation readings were recorded by initiating an oscillation for different gaps between the damping magnets (10mm, 20mm, 30mm, 40mm, 50mm). The gap was adjusted to get a set of readings each for underdamped, overdamped and critically damped motion and these data points were plotted in Figure 6.2.

Next, harmonic motion with driving was observed. For this, the magnet gap was set to 10mm. The banana plugs were attached to the Output of the 850 and the signal generator function was used for generating the driving. The signal was set to a sine wave and the drive voltage was set to 1V. The resonance frequency was found by plotting Lissajous figures (Figure 6.3 a,b,c) with output voltage on the x-axis and angle on y-axis. The Lissajous figure for resonance frequency is a circle on the parametric plot. Lastly, the amplitude responses were recorded for different driving frequencies and the resonance curve was plotted (Figure 6.4)

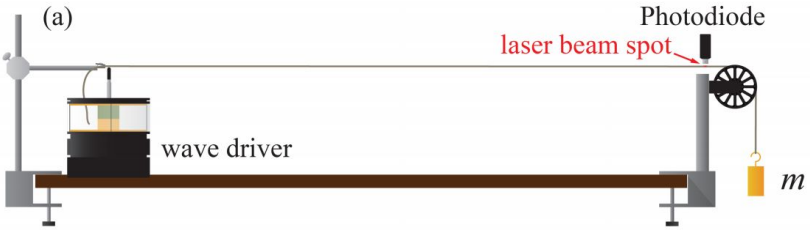

Figure 6.2 Experimental setup for studying the waves on a vibrating thick string. The wave driver drives the vibrations on the string and the photodiode records the laser beam spot on the string[1].

For the second part of the experiment, the apparatus was setup as demonstrated in Figure 6.2. The photodetector was positioned such that the laser light lit the top of the string in rest condition. The thick string was first weighed and its length was measured with and without the extra length that was clamped. The linear mass density was calculated by hanging three weights and measuring the length of the string. The wave driver and photodiode were connected to the DAQ. For measuring the velocity of the wave, a pulse was generated by the wave driver and using the graph plotted, the time interval for the pulse to travel the length of the string was noted. The Capstone setting for creating a sharp pulse was frequency =.25Hz and amplitude =1.0V. This was repeated for three weights (198.8g, 298.2g, 397.8g). For studying the standing waves, the heaviest mass was used to provide tension. The driving frequency was changed to find out the fundamental mode of resonance. Lissajous figures were graphed on the program to measure the exact frequency. The other modes of resonance were found by adjusting the frequency around the nth multiple of the fundamental node.

For the last part of this experiment, the string was driven at resonant frequencies for n=2,4 and 5 and the amplitude for photodiode oscillation was recorded. Then the string was constrained in the middle and and the amplitudes were recorded again.

Analysis

Harmonic Oscillation in a Physical Pendulum

For a physical pendulum of mass M at an angle of deviation θ, with its center of mass a distance l below the pivot, the torque due to gravity is given by:

$\tau_{grav} = -Mgl\ sin(\theta)$

The torque due to the attached spring is given by:

$\tau_{spring} = -B\ sin(\theta)cos(\theta)$

The magnets exert a damping force proportional to the tangential velocity of the pendulum.

$\tau_{\text{damping}} = -b\dot{\theta}$

Thus,

$$\begin{aligned} I\ddot{\theta} &= \sum_i \tau_i \\ &= -Mgl\sin(\theta) - B\sin(\theta)\cos(\theta) - b\dot{\theta} \end{aligned}$$

For small angular displacement ($\theta < 1rad$), $sin(\theta) \approx \theta$ and $cos(\theta) \approx 1$

$$\begin{aligned} I\ddot{\theta} &\approx -(Mgl + B)\,\theta - b\dot{\theta} \\ &= -k\theta - b\dot{\theta} \end{aligned}$$

This equation can be compared to equation:

$$m\ddot{x} = -kx - b\dot{x},$$

whose solution was derived in Experiment 5.

Thus by substituting $x \rightarrow \theta$ and $m \rightarrow I$ in the derived solution to the differential equation,

$$\theta(t) = Ae^{i\sqrt{\frac{k}{I}-\frac{b^2}{4I^2}}t} \times e^{-bt/2I}$$
$$= Ae^{i\omega_{\text{damped}}t} \times e^{-t/\tau}.$$

Similarly, the analogous equation for angular frequency is:

$$\omega_{\text{damped}} \equiv \sqrt{\frac{k}{I} - \frac{b^2}{4I^2}} = \sqrt{\omega_o^2 - \frac{1}{\tau^2}}$$

From the aforementioned equations time constant,

$$\tau \equiv \frac{2I}{b}$$

And the undamped resonance frequency is:

$$\omega_o \equiv \sqrt{k/I}$$

The regimes of oscillation as defined in the introduction occur when:

1) $\omega_0 > \frac{1}{\tau}$: Underdamped motion
2) $\omega_0 < \frac{1}{\tau}$: Overdamped motion
3) $\omega_0 = \frac{1}{\tau}$: Critically damped motion

The data points that were recorded for the three regimes of oscillation were plotted in Figure 6.2

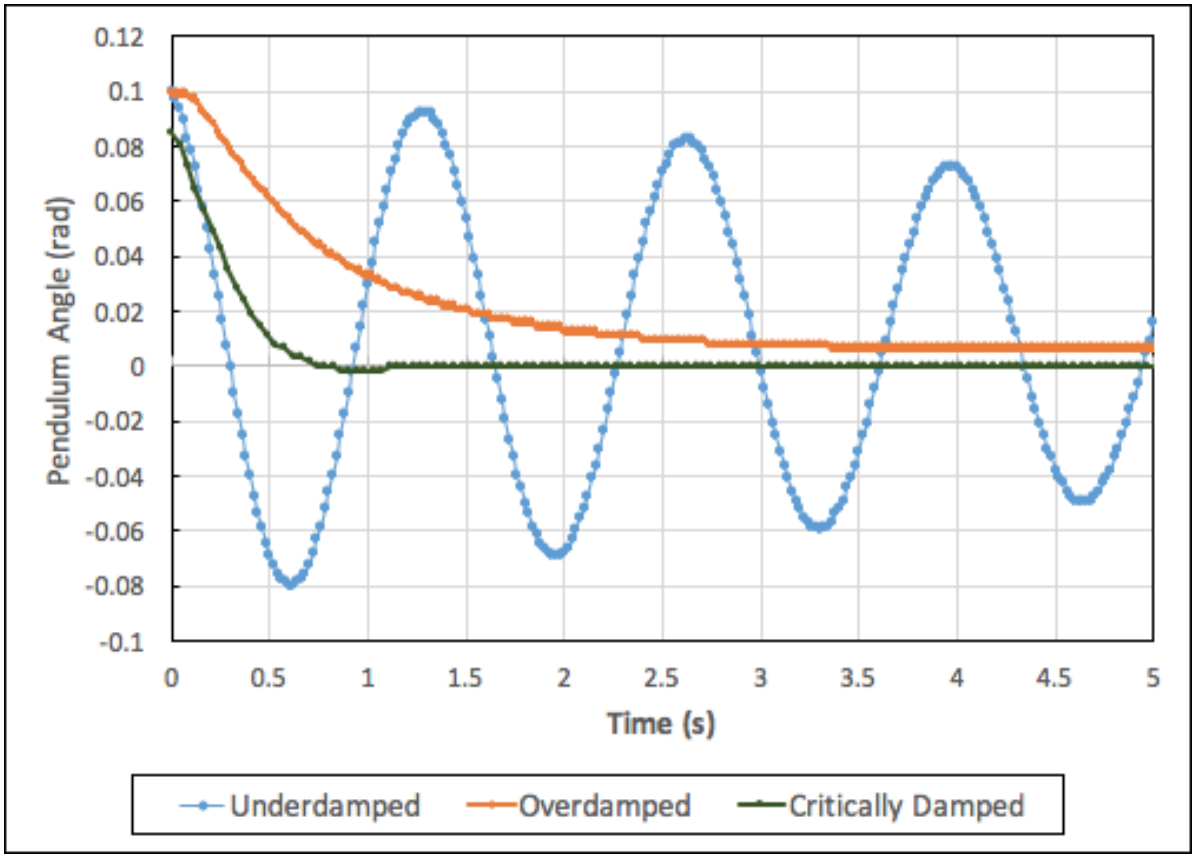

Figure 6.3 Pendulum angle versus time graph for underdamped, overdamped and critically damped oscillation. The three oscillations were started with almost the same displacement and it can be seen that the critically damped condition reaches 0 angular displacement fastest.

The underdamped motion was observed when there were no magnets to provide a damping force. Then five sets of readings were taken for separation of magnets 10mm, 20mm, 30mm, 40mm and 50mm.

Critically damped motion was observed when the separation between magnets was $16.0 \pm .5$ mm. Overdamped motion was observed when the separation was less than $16.0 \pm .5$

Undamped oscillation frequency was determined by zooming on the graph (Figure 6.3), noting the time of the maximas and first calculating the time period.

$T = 2.66 - 1.32 = 1.34 \pm .02s$

$f_0 = 1/T = .74 \pm .01Hz$

$\delta f_0 = f_0 \frac{\delta T}{T}$

The uncertainty in the Time period is equal to the interval of taking the readings(=.02s). By using error propagation, the uncertainty in frequency is .01Hz.

For driven oscillations, there is another term in the equation of motion which is dependent on the drive frequency ω_d

$$I\ddot{\theta} = -k\theta - b\dot{\theta} + C\cos(\omega_d t)$$

The resonance frequency of a damped driven system is the driving frequency at which the amplitude of oscillation is maximum. The expression for the resonant frequency can be obtained by solving the aforementioned differential equation and then differentiating the solution:

$$\omega_R = \sqrt{\omega_o^2 - 2\frac{1}{\tau^2}}.$$

The resonance frequency can also be found using the Lissajous figures (Figure 6.4 a,b,c). Figure 6.4c, which is almost a circle, was plotted at an amplitude of 1V and driving frequency of $.743 \pm .0005Hz$.

The damping time τ was found by measuring ratio of successive amplitudes in the undamped, undriven oscillation (Figure 6.3)

$$\tau = -\frac{T}{ln[\frac{F(t+T)}{F(t)}]}$$

By substituting the values, the mean damping time was found to be $12.4 \pm .3s$

The quality factor (Q) for such a system is defined by:

$$Q \equiv \frac{1}{2}\tau\omega_R$$

Using the values of τ and ω_R,

$Q = 4.588 \pm .002$

$\delta Q = |Q|\sqrt{(\frac{\delta\tau}{\tau})^2 + (\frac{\delta\omega}{\omega})^2}$

Q can also be defined as the ratio of resonant frequency and the width of the resonant curve (Figure 6.5)

$$Q \approx \frac{\omega_o}{\Delta\omega}$$

Using this formula,

$Q = \frac{.743}{.9} = 8 \pm 1$

The difference in the Q-factor values can be attributed to the small angle approximation and the uncertainty of determining the exact resonance width.

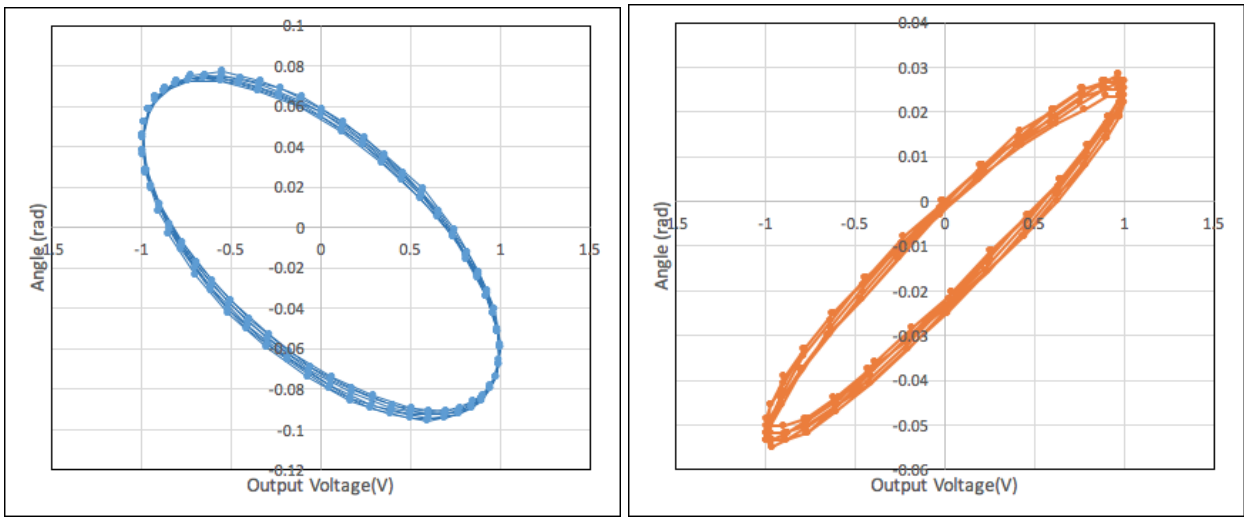

a) b)

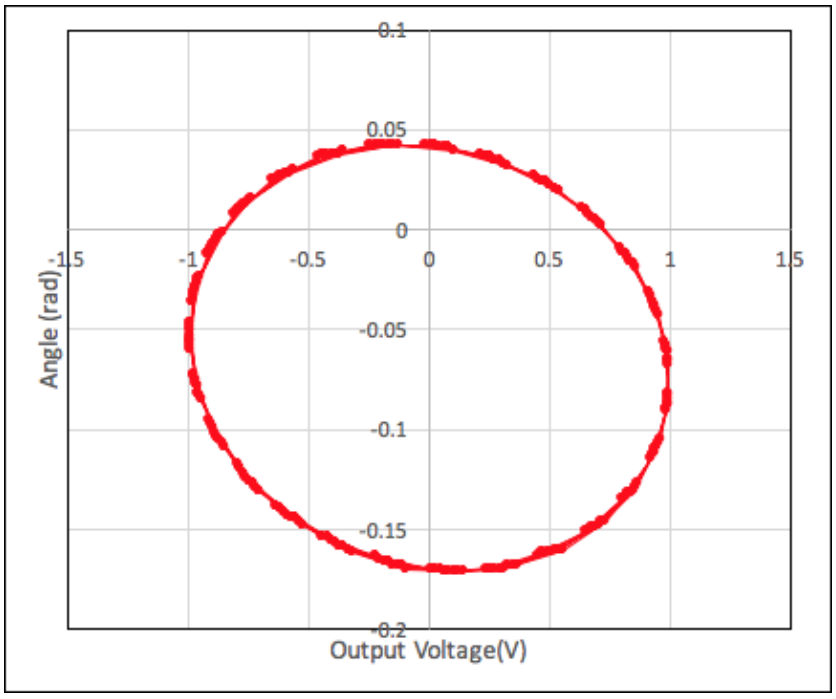

c)

Figure 6.4 Parametric plots of angle versus output voltage for a damped harmonic oscillator. These graphs show drive frequency a) above, b) below and c) exactly on resonance frequency.

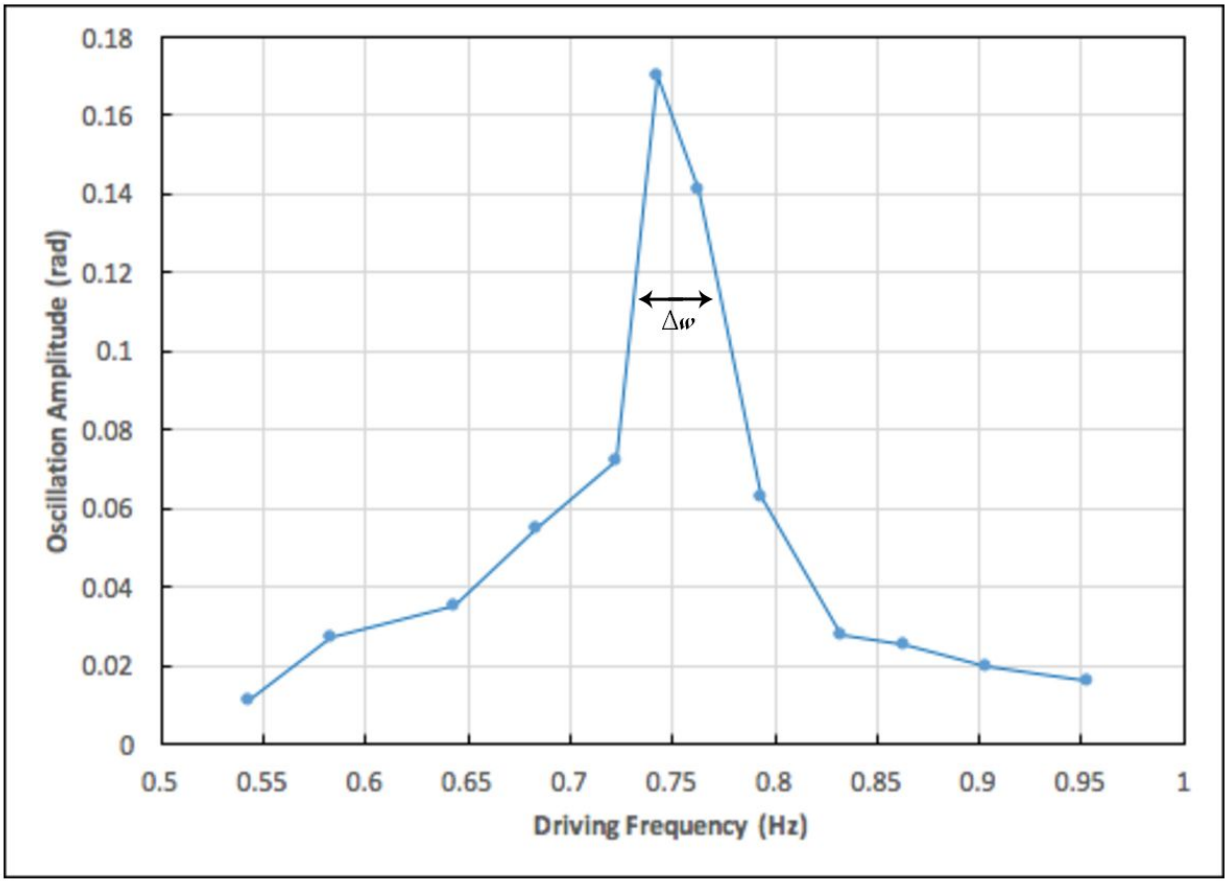

Figure 6.5 Resonance curve for driven oscillations. The points indicate the oscillation amplitude(radians) at the driving frequency. The points are joined by straight lines to form a Lorentzian shape. The resonance width is marked.

Oscillation of Waves on a vibrating string

For a string having tension T and linear mass density μ, the wave velocity is given by:

$$v = \sqrt{\frac{T}{\mu}}$$

The linear mass density changes as each weight on the string is attached. The mass of the string was:

$M_{string,\ total} = 14.3 \pm .05g$

Length of total string,

$L_{string,\ total} = 2.24 \pm .005m$

Length of used string (Total - clamped length)

$L_{string,\ used} = 2.03 \pm .005m$

$=> M_{string,\ used} = \frac{14.3}{2.24} * 2.03 = 12.95 \pm .05g = .01295 \pm .00005kg$

The mass of the string that hangs over the pulley is negligible when compared to the hanging weights thus it was neglected while calculating the mass.
The masses were hung over the pulley and the lengths were measured to calculate the linear mass density of the string. Table 6.1 shows the data recorded and calculations for obtaining the velocity of the wave moving on the string.

Mass (kg)	Tension (N)	Linear Mass Density (kg/m)	Wave Velocity (m/s)
$.1988 \pm .00005$	$1.9482 \pm .0005$	$.0079 \pm .0002$	$15.7 \pm .3$
$.2982 \pm .00005$	$2.9223 \pm .0005$	$.0076 \pm .0002$	$19.6 \pm .5$
$.3978 \pm .00005$	$3.8984 \pm .0005$	$.0074 \pm .0002$	$22.9 \pm .9$

Table 6.1 Calculations for wave velocity using the formula.

Uncertainty was calculated using
$\delta v = |v| \sqrt{(\frac{\delta T}{T})^2 + (\frac{\delta \mu}{\mu})^2}$

Wave velocity was also calculated using the light intensity versus time graph(Figure 6.6). The wave velocity is calculated by calculating twice the length of the string between pulley and clamp and dividing it by the difference in time of the sharp upward peaks of the graphs.

Mass (kg)	2*Distance between clamp and pulley - 2L (m)	Time interval between sharp peaks(s)	Wave Velocity (m/s) = Distance (2L)/Time
$.1988 \pm .00005$	$2.74 \pm .01$	$.174 \pm .0005$	$15.7 \pm .07$
$.2982 \pm .00005$	$2.74 \pm .01$	$.140 \pm .0005$	$19.5 \pm .09$
$.3978 \pm .00005$	$2.74 \pm .01$	$.120 \pm .0005$	$22.8 \pm .1$

Table 6.2 Calculations for wave velocity using time intervals between peaks of Figure 6.6 A), B) and C)
The uncertainty was calculated using
$\delta v = |v| \sqrt{(\frac{\delta L}{L})^2 + (\frac{\delta t}{t})^2}$
Where $\delta L = .01m$ and $\delta t = .0005s$

The results in Table 6.1 and Table 6.2 show that the calculated and measured wave velocities were the same within the uncertainties.
For the rest of the experiment the $.3978 \pm .00005$ kg mass was used to provide tension.

A)

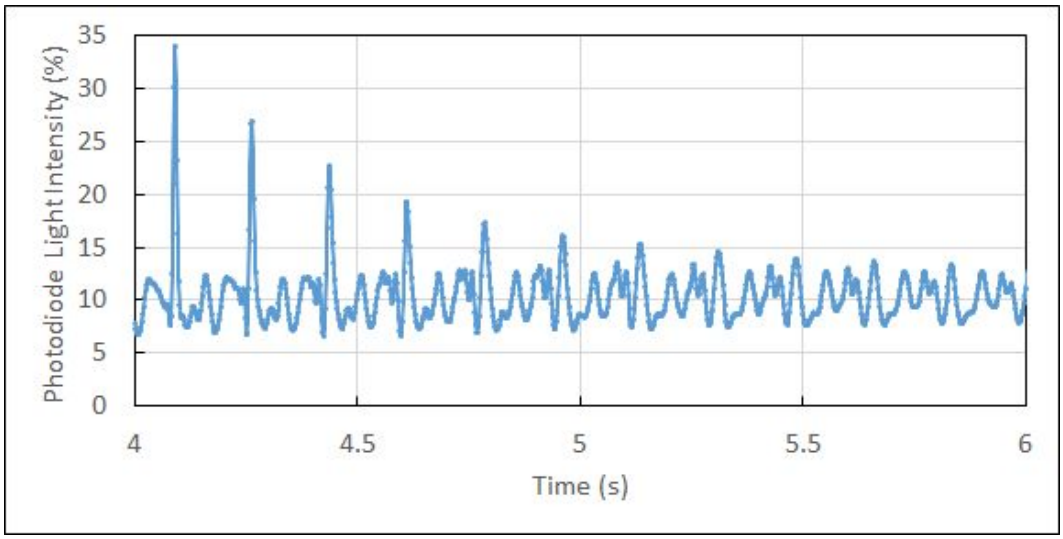

B)

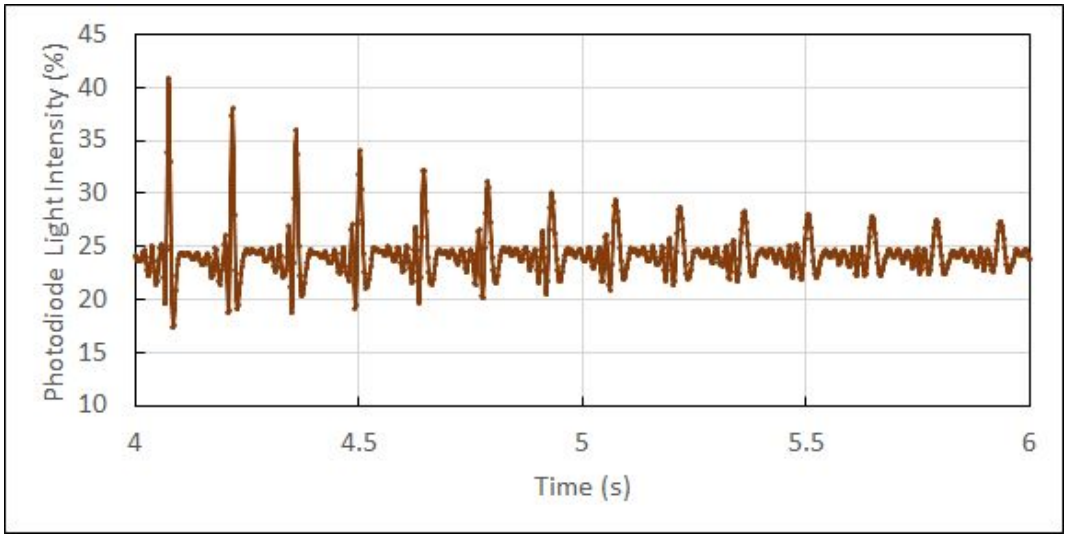

C)

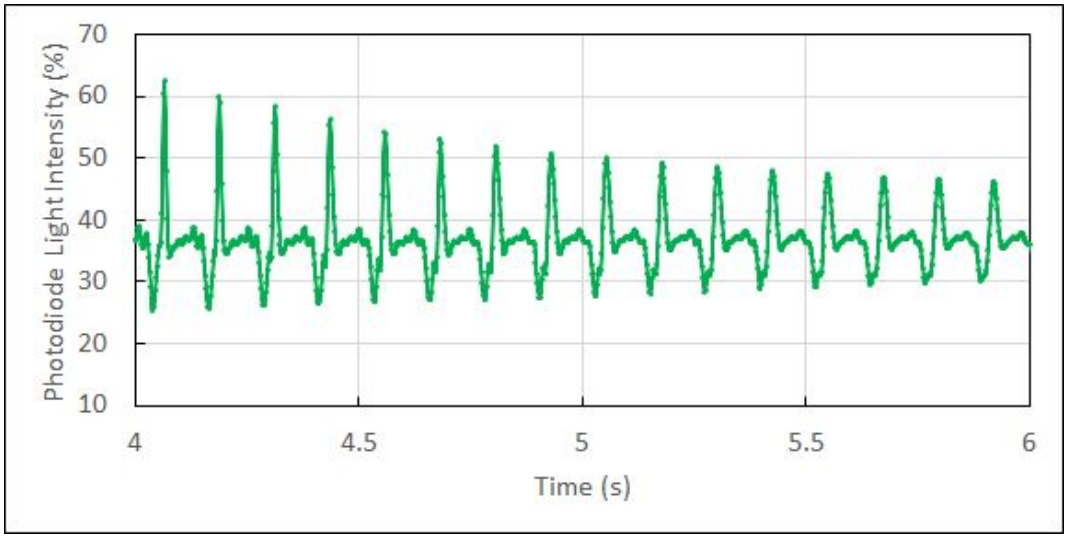

Figure 6.6 Zoomed plot of the pulse reflecting back and forth between the clamp and the pulley for A) 198.8g, B) 298.2g C)397.8g. The wave velocity is calculated by dividing the length of the string and dividing it by the difference in time of the sharp upward peaks of the graphs.

For identifying the precise fundamental resonance frequency, a parametric plot between light intensity and output voltage was graphed on the program. The drive frequency was tuned till the Lissajous figure was symmetric (Figure 6.7) This frequency was found to be $8.335 \pm .0005\,\text{Hz}$

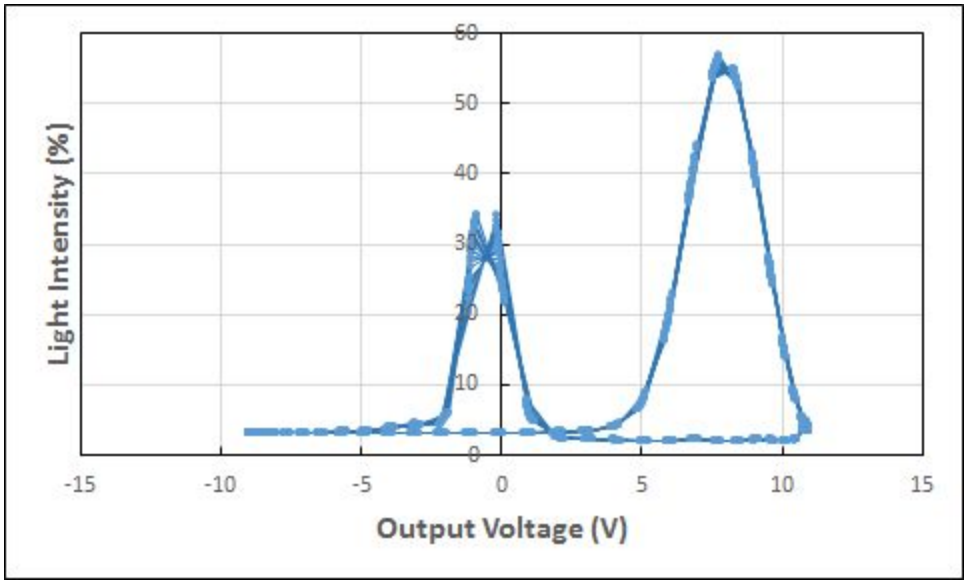

Figure 6.7 Light intensity versus output voltage parametric plot for drive frequency $8.335 \pm .0005\,\text{Hz}$

The expression for the frequency of the nth normal mode is:

$f(n) = \frac{nv}{2L}$

It was calculated using the experimentally velocity found in the experiment:

v=22.8± .1

2L= 2.74 ± .01m

$\delta f = |f| \sqrt{(\frac{\delta v}{v})^2 + (\frac{\delta L}{L})^2}$

Harmonic Number (n)	Measured Frequency (Hz)	Calculated Frequency(Hz)
1	$8.335 \pm .0005$	$8.3 \pm .1$
3	$25.005 \pm .0005$	$24.9 \pm .3$
6	$50.010 \pm .0005$	$49.8 \pm .6$
8	$66.680 \pm .0005$	$66.4 \pm .8$
9	$75.015 \pm .0005$	$74.7 \pm .9$

Table 6.3 Measured and calculated frequencies for nth modes. The calculated frequencies were found using the aforementioned formula for nth mode.

Table 6.3 demonstrates that the calculated frequencies are slightly lower than the measured velocities. However, the measured and calculated frequencies fall within the uncertainty range.

For studying the boundary effects the string was driven at a fixed amplitude for resonance frequencies of modes n=2,4,5 and the peak to peak size of the photodiode signal was recorded. Then a constraint was placed using a ring stand and post in the middle of the string and the signal amplitude was recorded again. These results are demonstrated in Table 6.4.

For the second and fourth mode the boundary was placed at a node. Theoretically, the string is divided into two parts and if the node is a boundary, both the parts of the string should have equal vibrations. The light intensity versus time graphs (Figure 6.8) for before and after putting the constraint were sinusoidal. For the fifth mode, the constraint was at an antinode so there was disturbance on the graphs.

n	Drive Frequency(Hz)	Signal Amplitude before constraint(%)	Signal Amplitude after constraint(%)
2	$16.670 \pm .0005 Hz$	50 ± 1	44 ± 1
4	$33.340 \pm .0005 Hz$	50 ± 1	41 ± 1
5	$41.675 \pm .0005 Hz$	58 ± 1	68 ± 1

Table 6.4 Drive frequency, signal amplitude before and after the constraint for n=2,4,5.

A)

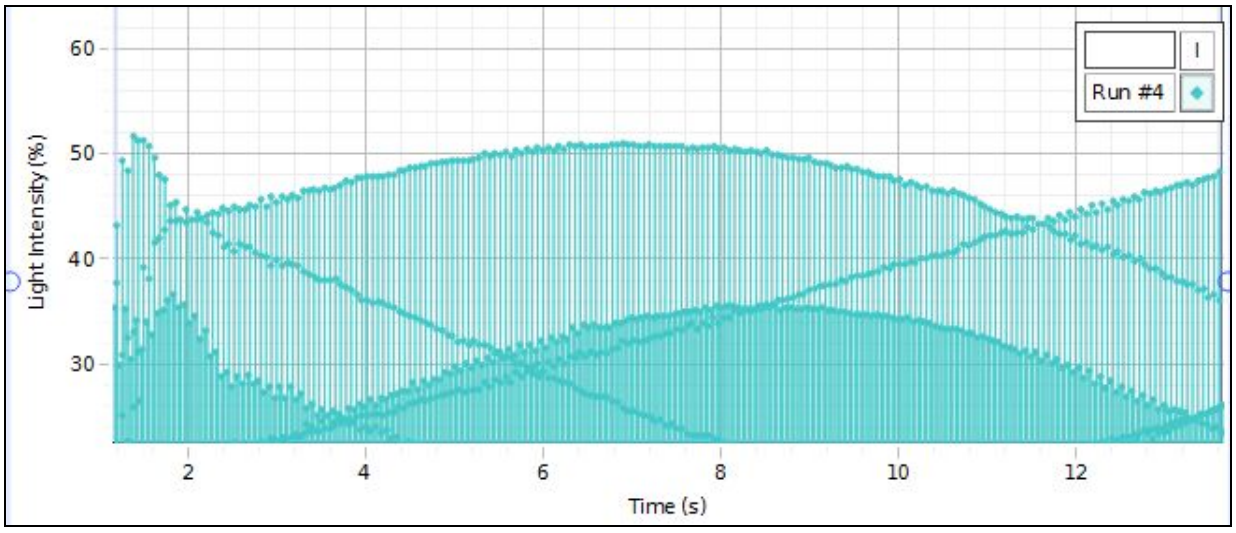

B)

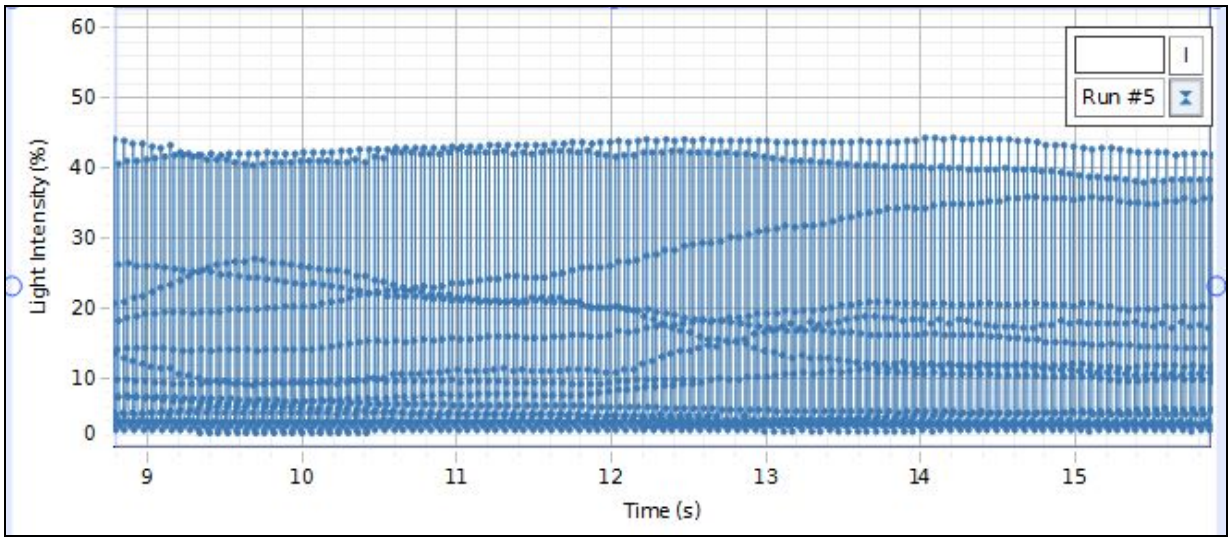

Figure 6.8 Capstone screenshot showing the peak to peak size of the photodiode signal for drive frequency 16.670Hz A) without the central constraint B) with the central constraint.

Conclusion

The objective of this experiment was to study harmonic motion of a physical pendulum and a wave on a vibrating string. The three regimes of harmonic motion—underdamped, overdamped and critically damped motion were investigated using an anchor-shaped aluminum pendulum and moving magnets to provide damping force. The magnet gap for critical damping in the pendulum was found by adjusting and observing the oscillations. The gap was $16.0 \pm .5$ mm. A driven oscillator was also studied and Lissajous figures (Figure 6.4) were used to measure the driven resonance frequency which was found to be $.743 \pm .0005 Hz$.

The Q-factor was calculated by finding the damping time. The calculated value of Q-factor was $4.588 \pm .002$. The resonance curve was plotted (Figure 6.5) by measuring the amplitude values at different drive frequencies. The Q-factor was calculated by dividing the resonant frequency by the resonance width. The difference in the Q-factor values obtained by the two methods can be attributed to the small angle approximation and the uncertainty of determining the exact resonance width. Furthermore, some systematic error was caused by the driver and the program since the Lissajous figures were not exactly the same for multiple runs with the same driving frequency.The first method is more precise. For getting a better value from the second method, the exact driving frequency should be found for $\frac{1}{\sqrt{2}}$ of the max amplitude.

For the wave on a vibrating string, the velocities were calculated for $.1988 \pm .00005 kg$, $.2982 \pm .00005$ kg, $.3978 \pm .00005$ kg hanging masses. The calculated velocities from the pulse graph (Figure 6.6) were $15.7 \pm .07$ m/s, $19.5 \pm .09$ m/s and $22.8 \pm .1$ m/s respectively. The velocities that were found using the formula by calculating the linear mass densities for different tensions were slightly greater than the measured values. This error might have been caused

because of neglection of tension due to the hanging string. To avoid this error, that value should have been taken into account. The fundamental frequency was experimentally determined by tuning the drive frequency till the Lissajous figure was symmetric. This frequency was found to be $8.335 \pm .0005$ Hz. The frequencies for mode 3, 6, 8, 9 were also found. The calculated frequencies from the formula were within the uncertainty range of measured values.

The results of investigating the boundary conditions for mode 2, 4 and 5 are demonstrated in Table 6.4. For mode 2 and 4, it was observed that the light intensity became less with the constraint but a sinusoidal motion was maintained. For mode 5, the light intensity became greater when the constraint was placed and the light intensity versus time graph showed disturbance. This was because for modes 2 and 4, the constraint was placed at nodes whereas it was placed at an antinode for mode 5. A possible source of systematic error is the constraint placed on the middle of the string. The ring and clamp constrained more than a single point and pushed the string slightly downwards due to which the peak-to-peak amplitude reading may not have been accurate. To avoid this error, a finer constraint system can be chosen such that the string is only stopped at a single point (node or antinode). For fixing the offset in the amplitudes, the amplitude difference can be recorded for cases with constraint and then be added to the values.

Bibliography

1. Campbell, W. C. *et al*. Physics 4AL: Mechanics Lab Manual (ver. May 15, 2016). (Univ. California Los Angeles, Los Angeles, California).